

Supplemental Information

The Determination of the Location of Contact Electrification-Induced Discharge Events

Sarah J. Vella^a, Xin Chen^a, Samuel W. Thomas III^a, Xuanhe Zhao^b, Zhigang Suo^b, and

George M. Whitesides^{*a,c}

^a*Department of Chemistry and Chemical Biology, Harvard University*

Cambridge, MA 02138

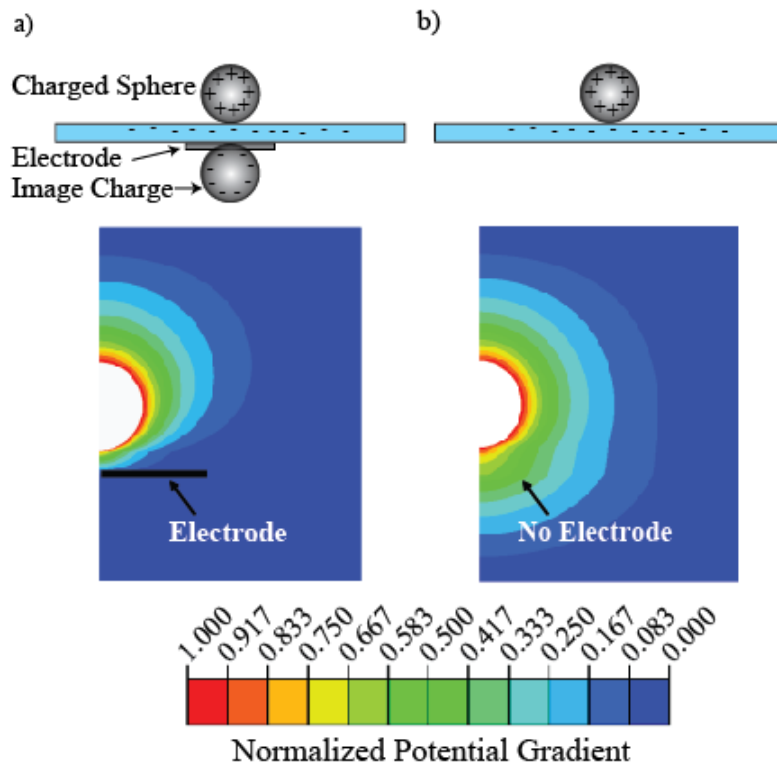
^b*School of Engineering and Applied Sciences, Harvard University,*

Cambridge, MA 02138

^c*Wyss Institute for Biologically Inspired Engineering, Harvard University,*

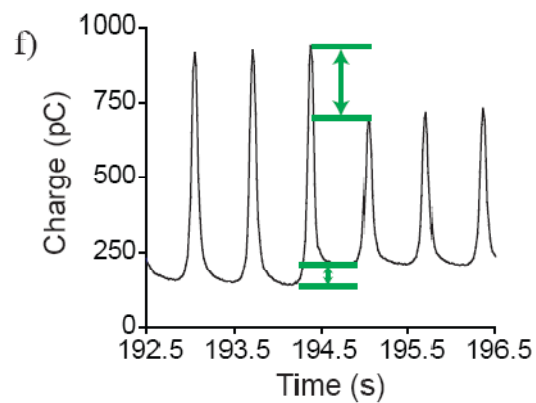
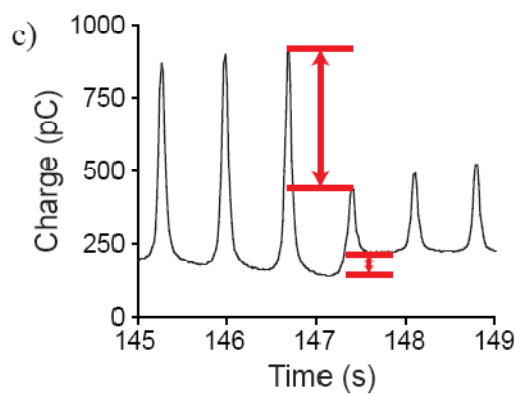
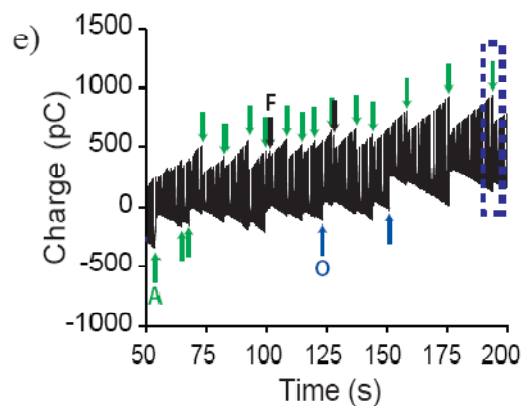
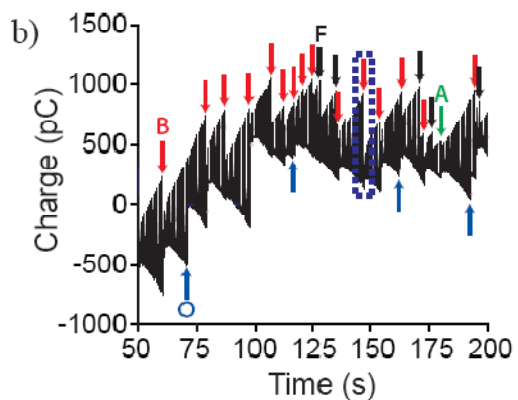
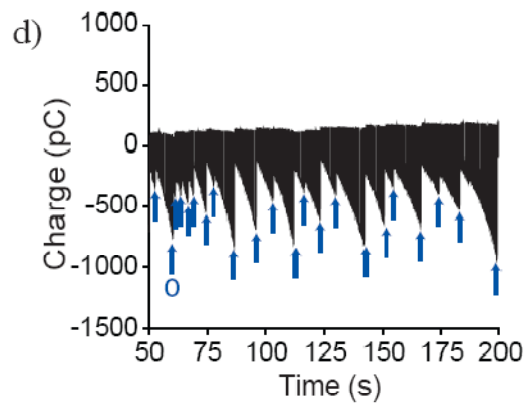
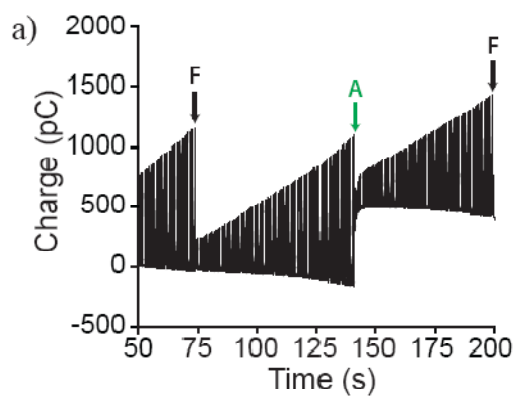
Cambridge, MA 02138

Figure S1 – The electric potential gradient from the surface of the sphere a) with an electrode and b) without an electrode.



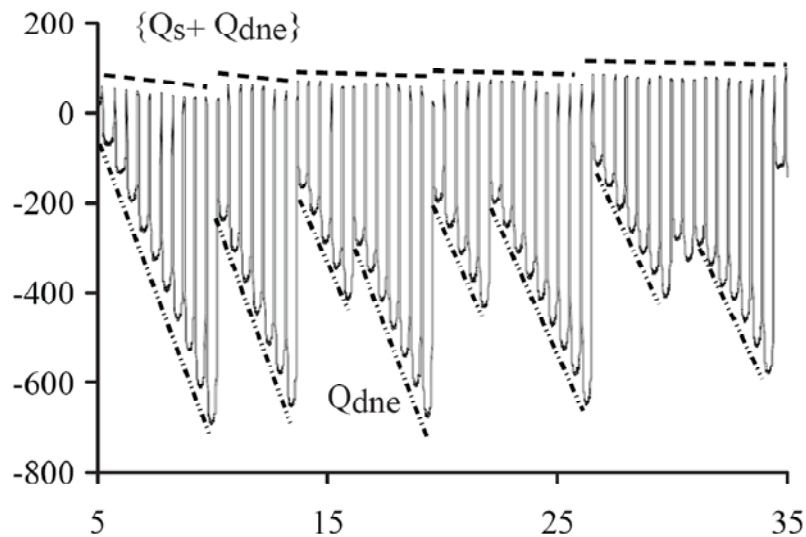
Using an axisymmetric model, the finite element software ABAQUS calculated the electric potential distribution around a charged sphere on a substrate; the relative dielectric constant for air was 1, and for the polymer substrate was 4. The electric potential gradient (i.e. electric field) below the charged ball was much higher with a grounded electrode beneath the substrate (Figure S1a), than without an electrode (Figure S1b). This larger electric field increased the probability of discharge when the sphere was above or close to the electrode.

Figure S2 – A steel sphere ($d = 3.2$ mm) rolling on a PS Petri dish ($T \sim 25^\circ\text{C}$, $\text{RH} < 10\%$): a) before plasma oxidation; b) after plasma oxidation of Zone **B** (as shown in Scheme 1) – 15 of the 25 discharges *shown* occurred in Zone **B**; c) an expanded view of the highlighted data in the blue box in (b) showing that the discharge was a “Peak” followed by “Baseline” disruption indicative of a Zone **B** discharge; d) after plasma oxidation of Zone **O** – 22 of the 22 discharges *shown* occurred in Zone **O** e) after plasma oxidation of Zone **A** – 16 of the 20 discharges *shown* occurred in Zone **A** (green arrows); f) an expanded view of the highlighted data in the blue box in (e) showing that the discharge is a “Baseline” followed by a “Peak” disruption indicative of a Zone **A** discharge.



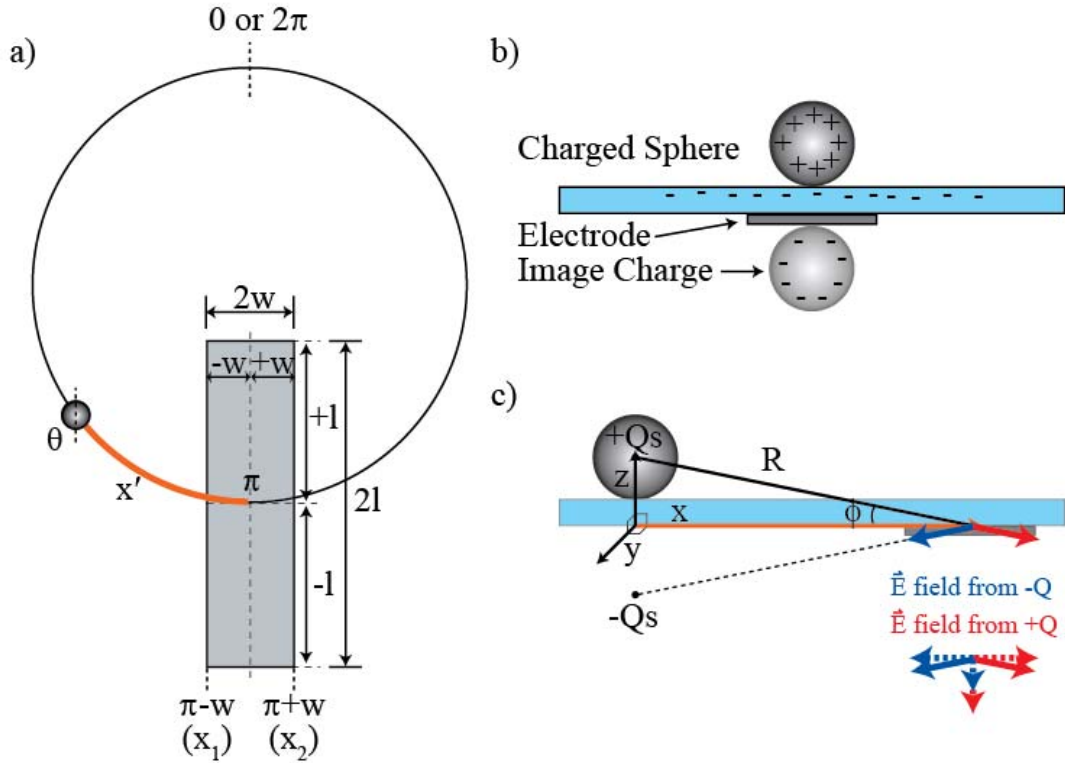
For samples that only had a region plasma oxidized, the charging occurred almost entirely when the sphere rolled on the oxidized region of the PS dish. Figure S3 shows data from a steel sphere rolling on a plasma-oxidized PS Petri dish where the oxidized zone was positioned over the electrode (Zone **O**); both the steep slope of the baseline (Q_{dne}), and the lack of increase in $\{Q_s + Q_{dne}\}$, indicated that charge separation occurred almost exclusively over Zone **O**. Although this charging trend was not as apparent in the data traces from a steel sphere rolling on a PS dish in which only Zone **B**, or Zone **A**, had been plasma oxidized, we assumed that charge separation also occurred more rapidly over the treated regions. The unequal charging rate over the surface must also result in more charge on the treated region than the untreated region.

Figure S3 – 25s of data from a steel sphere ($d = 3.2$ mm) rolling on a Zone O plasma-oxidized PS Petri dish. Both the steep slope of the baseline (Q_{dne} , $- \bullet \bullet$) and the lack of increase in $\{Q_s + Q_{dne}\}$ ($- - -$) indicate that charge separation occurred almost exclusively over Zone O.



Derivation of Eq. 10.

Figure S4



We assumed that the difference between x' and x was negligible.

$$\bar{E} = \frac{Q}{4\pi\epsilon_0 R^2}$$

$$R^2 = z^2 + x^2 + y^2$$

$$R = \sqrt{z^2 + x^2 + y^2}$$

$$\bar{E} = \frac{Q}{4\pi\epsilon_0 (z^2 + x^2 + y^2)}$$

Since: $\sin \phi = \frac{z}{R}$

z component of \bar{E}

$$\bar{E}_z = \bar{E} \sin \phi = \frac{Qz}{4\pi\epsilon_0 R^3} = \frac{Qz}{4\pi\epsilon_0 (z^2 + x^2 + y^2)^{3/2}}$$

Since there are 2 z components (one from the real charge and one from the image charge):

$$\vec{E}_{tot} = \vec{E}_z - (-\vec{E}_z) = 2\vec{E} \sin \phi = \frac{Qz}{2\pi\epsilon_o(z^2 + x^2 + y^2)^{3/2}}$$

$$Q_e = \int A_{electrode} (\epsilon_o \vec{E} dy dx), \text{ A is the surface area of the electrode}$$

$$Q_e = \epsilon_o \int_{x_1}^{x_2} \int_{y_1}^{y_2} \vec{E}_{tot} dy dx$$

Here the limits y_1 and y_2 are $-l$ and $+l$, and x_1 and x_2 are $(\pi-w-\theta)$ and $(\pi+w-\theta)$

$$Q_e = \frac{Q_s z}{2\pi} \int_{\pi-w-\theta}^{\pi+w-\theta} \int_{-l}^{+l} \frac{1}{(z^2 + x^2 + y^2)^{3/2}} dy dx$$

By symmetry $-l$ to $+l$ is $2l$:

$$Q_e = \frac{Q_s z}{\pi} \int_{\pi-w-\theta}^{\pi+w-\theta} \int_0^{+l} \frac{1}{(z^2 + x^2 + y^2)^{3/2}} dy dx$$

Integrate over y:

$$\begin{aligned} & \int_0^{+l} \frac{1}{(z^2 + x^2 + y^2)^{3/2}} dy \\ &= \frac{Q_s z}{\pi(x^2 + z^2)} \left(\frac{y}{\sqrt{y^2 + x^2 + z^2}} \right) \Big|_0^l \\ &= \frac{Q_s z}{\pi(x^2 + z^2)} \left(\frac{l}{\sqrt{l^2 + x^2 + z^2}} \right) \end{aligned}$$

Since: $l \gg x^2 + z^2$,

$$\text{Therefore: } Q_e = \frac{Q_s z}{\pi} \int_{\pi-w-\theta}^{\pi+w-\theta} \frac{1}{(x^2 + z^2)} dx$$

Integrate over x :

$$\begin{aligned} Q_e &= \frac{Q_s}{\pi} \left[\arctan\left(\frac{x}{z}\right) \right] \Big|_{\pi-w-\theta}^{\pi+w-\theta} \\ &= \frac{Q_s}{\pi} \left[\arctan\left(\frac{\pi+w-\theta}{z}\right) - \arctan\left(\frac{\pi-w-\theta}{z}\right) \right] \\ &= \frac{Q_s}{\pi} \left[\arctan\left[-\left(\frac{\theta-\pi-w}{z}\right)\right] \right] - \left[\arctan\left[-\left(\frac{\theta-\pi+w}{z}\right)\right] \right] \\ &= \frac{Q_s}{\pi} \left[\arctan\left(\frac{\theta-\pi+w}{z}\right) - \arctan\left(\frac{\theta-\pi-w}{z}\right) \right] \end{aligned}$$